Exosomal miR-6126 as a novel therapeutic target for overcoming resistance of anti-cancer effect in hepatocellular carcinoma

BMC Cancer

RESEARCH

Open Access

Exosomal miR-6126 as a novel therapeutic target for overcoming resistance of anti-cancer effect in hepatocellular carcinoma

Hyemin Hwang[1†], Jimin Kim[1†], Tae-Hun Kim[2], Yeonju Han[1], Dayoung Choi[1], Sua Cho[1], Seunghwan Kim[1], Sanghee Park[1], Taehyun Park[1], Filippo Piccinini[3,4], Won Jong Rhee[5], Jae-Chul Pyun[2] and Misu Lee[1,6*]

Abstract

Background Hepatocellular carcinoma (HCC) stands as the sixth most prevalent cancer globally, presenting a substantial health challenge, particularly due to late-stage diagnoses that limit treatment effectiveness. Sorafenib, a multi-kinase inhibitor, is the primary chemotherapeutic agent for advanced HCC, but it only extends survival by 2–3 months. However, drug resistance remains a major clinical challenge, necessitating the exploration of new molecular mechanisms, including the role of microRNAs (miRNAs) in sorafenib resistance. In this study, we aimed to identify miRNAs within exosomes derived from sorafenib-resistant HCC cells to elucidate the molecular mechanisms underlying resistance.

Methods Sorafenib-resistant cells were generated by culturing the human HCC cell line Huh7 in a medium containing 20 μM sorafenib for six months. Exosomes were isolated from the conditioned medium 24 h before cell harvest using exosome-depleted serum medium. miRNA sequencing and western blotting were used to analyze the expression profiles of exosomal miRNAs and proteins, respectively. pH measurement was performed to assess pH changes in response to sorafenib treatment and miRNA modulation.

Results A total of 180 exosomal miRNAs were found to be dysregulated between sorafenib-treated control Huh7 (Huh7S) and sorafenib-resistant Huh7 (Huh7RS) cells, as well as between untreated control Huh7 and Huh7RS cells. Among these, miR-6126 was significantly downregulated in Huh7RS cells compared to Huh7S cells. Functional studies using 2-dimensional (D) and 3D cell culture systems revealed that miR-6126 overexpression reduced sorafenib resistance in Huh7RS cells, while its inhibition increased resistance in Huh7 cells. miR-6126 downregulated key proteins involved in cancer stem cell maintenance, such as CD44 and HK2. Furthermore, the pH level was elevated in cells overexpressing miR-6126 following sorafenib treatment, whereas inhibiting miR-6126 resulted in a lower pH.

Conclusions Exosomal miR-6126 plays a pivotal role in sorafenib resistance and tumorigenesis, highlighting its potential as a novel therapeutic target for overcoming drug resistance in HCC.

Keywords Hepatocellular carcinoma, Exosomes, MicroRNA, Drug resistance, Cancer metabolism

†Hyemin Hwang and Jimin Kim contributed equally to this work.

*Correspondence:
Misu Lee
misulee@inu.ac.kr
Full list of author information is available at the end of the article

Background

Liver cancer, primarily presenting as hepatocellular carcinoma (HCC), is the sixth most common cancer globally and the second leading cause of cancer-related deaths. Despite the available treatment modalities, such as surgical resection, ablation, and chemoembolization, high rates of metastasis and frequent postsurgical recurrence contribute to the poor prognosis of patients with HCC [1, 2]. Sorafenib, a multi-kinase inhibitor, remains the standard treatment for advanced HCC. It exerts its antitumor effects by suppressing tumor cell proliferation through the inhibition of Raf-1, B-Raf, and kinase activity within the Ras/Raf/MEK/ERK signaling pathway [3]. In addition to its anti-proliferative effects, sorafenib suppresses angiogenesis by inhibiting platelet-derived growth factor receptor (PDGFR-β) and vascular endothelial growth factor receptor (VEGFR) [4, 5]. Sorafenib has shown significant benefits in treating advanced HCC, with a median time to progression of 4.2 months and an overall survival of 9.2 months [6]. However, only approximately 30% of patients benefit from sorafenib, and even they typically develop drug resistance within 6 months [7].

Elevated glycolysis (also known as the Warburg effect) is essential for the rapid proliferation of cancer cells [8]. This heightened glycolytic activity leads to the generation of high levels of lactate, which subsequently increases the intracellular proton (H^+) concentration. Furthermore, glutaminolysis acts as an additional pathway for ATP production and contributes to the production of lactate and H^+ in cancer cells, thereby promoting resistance to radiation and chemotherapy [9, 10]. In liver cancer stem cells, this metabolic switch enhances their resistance to sorafenib, and inhibiting this switch has been shown to increase sorafenib sensitivity [11].

Extracellular vesicles (EVs), nanosized membrane vesicles containing RNA, plasmids, metabolites, or other small molecules, are released by all cells (stromal and tumor cells) into the extracellular space [12, 13]. Among EVs, exosomal miRNAs contributing to tumor proliferation, angiogenesis, and metastasis have emerged as key players in the reprogramming of tumors. For instance, exosomal miR-103 enhances vascular permeability and tumor metastasis in HCC and is considered a potential therapeutic target [14]. Exposure of tumor cells to various anticancer agents promotes the secretion of exosomes from tumor cells, which alters drug sensitivity by delivering cargo mRNAs and miRNAs into recipient cells [15, 16]. Therefore, exploration of the roles of exosomal miRNAs as potential regulators of sorafenib resistance has gained increased interest. Recently, Ji et al. [16] demonstrated that miR-486-3p mediates sorafenib resistance by targeting EGFR, whereas Feng et al. [17] showed that miR-25 enhances autophagy and promotes sorafenib resistance. Based on these studies, we hypothesize that specific miRNAs within exosomes derived from sorafenib-resistant HCC cells contribute to the development of drug resistance and tumor progression.

To test this hypothesis, in this study, we aimed to investigate the expression profile of exosomal miRNA in sorafenib-resistant HCC cell lines and assess the functional role of these dysregulated miRNAs on sorafenib resistance and tumorigenesis. This study will uncover potential molecular targets for overcoming drug resistance in HCC.

Methods

Chemicals

Sorafenib was purchased from Santa Cruz (Dallas, TX, USA), dissolved in dimethyl sulfoxide (DMSO) (Sigma Aldrich, St. Louis, MO, USA) at a concentration of 10 mM, and stored at − 80 °C.

Cell culture

Huh7 and SK-Hep1 cells, human HCC cell lines, were purchased from the Korean Cell Line Bank (Seoul, South Korea) and cultured in Dulbecco's modified Eagle's medium (DMEM; Gibco, Thermo Fisher Scientific, Wilmington, DE, USA) supplemented with 10% (v/v) heat-inactivated fetal bovine serum (FBS; Hyclone, Marlborough, MA, USA) and 1% (v/v) penicillin-streptomycin (Gibco, Thermo Inc.). Cells were incubated in an incubator with 5% CO_2 at 37 ℃. Sorafenib-resistant HCC cells (Huh7R) were generated by continuous exposure of Huh7 cells to 1–20 μM sorafenib for 6 months and the IC_{50} was evaluated. Reduction of cell viability was much lower in Huh7R cells compared with Huh7 cells (IC_{50} of Huh7R = 32.31 μM, and IC_{50} of Huh7 = 14.86 μM, Additional File 1; Fig. S1). All cells were confirmed to be free from contamination using the standard mycoplasma test. To generate three-dimensional (3D) spheroids, cells were mixed with either a mimic or inhibitor in culture medium and seeded at 1.5×10^5 cells/ml into Costar ultra-low attachment 96-well plates (Corning, Darmstadt, Germany). The plates were centrifuged at 179 × *g* for 1 min to promote the formation of a single spheroid per well. The morphology and size of the spheroids were monitored using phase-contrast microscopy.

Exosome isolation

Exosomes were isolated from the cell culture medium using the ExoQuick-TC kit (System Biosciences, Palo Alto, CA, USA) according to the manufacturer's protocol. Briefly, cells were seeded into a cell culture plate (1.0×10^5/mL). The medium was replaced with an exosome-depleted medium containing 10% (v/v) exosome-depleted FBS (Gibco) and 1% (v/v)

penicillin-streptomycin. After 24 h, the medium was collected and centrifuged at 3,000 × *g* at 4 ℃ for 30 min. ExoQuick-TC reagent (SBI) was added to 20% of the total volume of the supernatant and then resuspended smoothly to obtain a homogenous solution. After 24 h of additional incubation at 4℃, the mixture was centrifugated at 1,500 × *g* at 4 ℃ for 15 min and the supernatant was removed. Additional centrifugation was performed for 5 min to completely aspirate any remaining liquid. The exosome pellet was resuspended in 1× phosphate-buffered saline (PBS) and used for further studies.

Characterization of exosome

Dynamic light scattering (DLS) and zeta potential were measured using ZetaPALS® (Brookhaven Instruments, Holtsville, NY, USA). For both analyses, exosome samples were mixed and diluted to a final volume of 2 mL with PBS. Zeta potential analysis was conducted using the Smoluchowski model to evaluate the surface charge of the exosomes [18]. To confirm the successful isolation and labeling of exosomes, the ExoGlow™ Membrane EV Labeling Kit (SBI) was used according to the manufacturer's instructions. Specifically, a labeling mixture containing 6 µL reaction buffer and 1 µL fluorescent dye was prepared. Fifty micrograms of exosomes derived from Huh7, sorafenib-treated Huh7 (Huh7S), and sorafenib-treated Huh7R cells (Huh7RS) cells were added to the mixture and incubated at ambient temperature for 30 min. Subsequently, the free and unlabeled dye was removed by adding 0.35× volume of ExoQuick-TC reagent to each sample, followed by incubation at 4 °C for 1 h. For exosome uptake studies, normal Huh7 cells were seeded into a 6-well plate at a density of 2.5×10^5cells/mL onto poly-L-lysine-coated coverslips and allowed to adhere for 24 h. These cells were then incubated with labeled exosomes for 18 h. After incubation, the cells were fixed with 4% paraformaldehyde for 20 min and subsequently stained with Hoechst 33,258 (Invitrogen) to visualize nuclei. The cellular uptake of EV membrane-labeled exosomes was analyzed using an Olympus BX53 microscope equipped with Olympus CellSens software (Carl Zeiss Microscopy, Jena, Germany).

Western blotting

Cells or exosomes were lysed using RIPA buffer (Biosesang, South Korea) with 100× Xpert Protease Inhibitor Cocktail (GeneDepot, Katy, TX, USA). BCA assay was performed to determine the concentration of proteins using the Pierce BCA Protein Assay Kit (Takara Bio Inc., Otsu, Japan). For western blotting, 10 µg of proteins were separated on 10% SDS-PAGE gels, and transferred from the gels to PVDF membranes (Merck Millipore, Darmstadt, Germany) for 1 h 10 min. Thereafter, the membranes were blocked with 5% skim milk in TBST for 1 h. Primary antibodies were diluted with 3% BSA in TBST and used to determine protein expression. Anti-rabbit or anti-mouse secondary antibodies (Gentex, Irvine, CA, USA) were additionally used for the detection. ECL analysis was performed using ChemiDoc XRS (Bio-Rad, Hercules, CA, USA) for the digital visualization of chemiluminescent western blots. The experiments were replicated at least three times, and all showed similar results. The antibodies used are summarized in Additional File 1; Table S1. To quantify the blots, Image Lab (Bio-Rad) was used for image analysis.

miRNA sequencing and real-time qPCR

Total RNA was extracted using an RNeasy Mini Kit (Qiagen, Hilden, Germany), according to the manufacturer's protocol, and quantified using a NanoDrop spectrophotometer (DeNovix, Wilmington, DE, USA). miRNA sequencing was performed by EBIOGEN, Inc. (Seoul, Korea). To determine the expression levels of miRNAs in exosomes, RT-qPCR was performed using a C1000TM Thermal Cycler (Bio-Rad Laboratories, Hercules, CA, USA) and a miRCURY LNA SYBR Green PCR Kit (Qiagen) following the manufacturer's protocol. Complementary DNA (cDNA) of the miRNAs was synthesized from 10 to 20 ng of total RNA using the miRCURY LNA RT Kit (Qiagen, Hilden, Germany), according to the manufacturer's protocol. miRNA expression was normalized to that of rRNA. Target miRNAs hsa-miR-6126, hsa-miR-148a-3p, hsa-miR-1290, hsa-miR-4516, and rRNA were validated using the miRCURY LNA miRNA PCR Assay (Qiagen). The miRNA expression levels were normalized to those of rRNA in the corresponding cDNA samples.

Transfection and treatment

Cells were seeded into 6-well plates containing Opti-Minimal Essential Medium (Opti-MEM; Gibco) for reverse transfection and then treated with a miRNA mimic or inhibitor. Commercial miR-6126 mimics and inhibitors were purchased from Bioneer (Daejeon, South Korea). Lipofectamine RNAiMAX Transfection Reagent (Invitrogen, Carlsbad, CA, USA) was used for transfection following the manufacturer's instructions. As a negative control, a commercial miRNA mimic was synthesized by Genolution (Seoul, South Korea). After 48–72-h incubation, the cells were harvested for further analysis.

Measurements of cell viability and pH level

Cells were seeded into 96-well plates at a density of 5.0×10^3 cells/well and incubated for 24 h up to approximately 70% confluency. The plates were then treated with

various concentrations of sorafenib. After 48 h, 10 mL of Cell Counting Kit-8 (Dojindo Laboratories, Kumamoto, Japan) was added to each well and incubated for 1 h in an incubator at 37 ℃ and 5% CO_2. Cell viability was determined by measuring the absorbance at 450 nm using a Spectra Max190 microplate reader (Molecular Devices, Sunnyvale, CA, USA). To assess the level of pH, Huh7 cells were transfected with a mimic control, miR-6126, or a miR-6126 inhibitor for 24 h, followed by incubation with the pHrodo Red dye (Thermo Fisher Scientific). The pH measurements were performed as described in a previous study [19].

Statistical analysis

GraphPad Prism (GraphPad Software Inc., San Diego, CA, USA) was used for statistical analyses. Comparisons between each condition were performed using one-way analysis of variance (ANOVA) with Tukey's multiple comparisons tests and unpaired t-tests. All data are expressed as means ± SD (range) and statistical significance was set at $P < 0.05$.

Results

Extraction of exosomes (EV) from Huh7 cells with different sensitivity of sorafenib

Recent findings by Gao et al. have shown that Huh-7 cells are among the most sensitive HCC cell lines to Sorafenib, ranking in the top four of 14 different lines assessed for drug sensitivity [20]. This sensitivity makes Huh-7 an excellent model for studying Sorafenib resistance, as it allows for the identification of miRNAs and other molecular factors that contribute to the development of resistance in a previously sensitive cell line. Thus, we generated Sorafenib-resistant cells using Huh7. Evaluation of the expression of proliferation, glycolysis, and stem-related proteins in Huh7, Huh7S and Huh7RS cells revealed elevated levels of phospho-ERK 1/2 (p-ERK1/2), glycolysis-related proteins (HK2), and cancer stem cell marker (CD44) in Huh7RS cells compared to those in Huh7 and also Huh7S cells (Fig. 1A-B and Additional File 1; Fig. S2). Additionally, the level of pH was also reduced in Huh7RS cells compared with those in Huh7 and Huh7S cells (Fig. 1C). Exosomes were extracted from Huh7, Huh7S, and Huh7RS cells (Fig. 1A) and analysis of the expression of the EV markers using western blotting revealed higher expression of CD63 and TSG101, the positive markers of exosomes, in exosomal proteins than those in cell lysates, whereas calnexin, a negative exosomal marker, was clearly expressed in lysate proteins but not in exosomal proteins (Fig. 1D). EVs from Huh7, Huh7S, or Huh7RS cells were labeled with a fluorescent dye and subsequently added to the control Huh7 cells. Fluorescence was observed in all Huh7 cells after treatment with exosomes from three conditions (Fig. 1E), Furthermore, DLS and zeta potential assessments showed that the size of exosomes derived from Huh7, HuhS, and Huh7RS ranged from 200 to 300 nm with slight variations between each cell type (Fig. 1F). The zeta potential ranged between −16.7 mV and −20.1 mV (Fig. 1G). Together, these findings confirmed the successful isolation of exosomes from Huh7, Huh7S, and Huh7RS.

Identification of exosomal miRNAs derived from sorafenib-resistant HCC cells

After the successful extraction of exosomes from Huh7, Huh7S, and Huh7RS cells, the differential expression of miRNAs across the cells was analyzed using miRNA array (fold change > 1.5). A total of 200 miRNAs were dysregulated in Huh7S cells compared with those in control Huh7 cells, whereas 199 miRNAs were dysregulated in Huh7RS cells compared with those in Huh7S cells (Fig. 2A and B). Furthermore, KEGG pathway enrichment analysis revealed that the 20 dysregulated miRNAs common between Huh7S and Huh7 cells (blue area in Venn diagram) were associated with the phospholipase D signaling pathway, miRNAs in cancer, and HCC (Fig. 2C). Meanwhile, the 47 dysregulated miRNAs common between Huh7RS and Huh7S cells (red area in Venn diagram) were involved in the AMPK, PI3K-AKT, and mTOR signaling pathways, as well as in the pathways regulating stem cells (Fig. 2D). Moreover, we identified 140 miRNAs differentially expressed between Huh7S and Huh7 cells and Huh7RS and Huh7S cells, which have been implicated in PI3K-AKT signaling, focal adhesion, regulation of the actin cytoskeleton, and the MAPK signaling pathway (Fig. 2E). These finding suggest distinct miRNA expression profiles after the acquisition of sorafenib resistance.

Downregulated miRNAs derived from sorafenib-resistant HCC cells

Among the 140 miRNAs that were differentially expressed between Huh7S vs. Huh7 and Huh7RS vs. Huh7S cells, the expression of miR-4516, miR-6126, and miR-148-3p, which are related to tumorigenesis, was verified by qRT-PCR using exosomal miRNAs. Consistent with the miRNA array results, exosomal miRNAs that were upregulated after sorafenib treatment in control Huh7 cells were significantly downregulated in Huh7RS cells, similar to their expression levels in Huh7 cells without sorafenib treatment (Fig. 3A-C). Additionally, miR-4516, miR-6126, and miR-148-3p were upregulated in miRNAs derived from control Huh7 cells after sorafenib treatment, whereas no change in the expression of these miRNAs was observed in Huh7R cells after sorafenib treatment (Additional File 1; Fig. S3A–S3C).

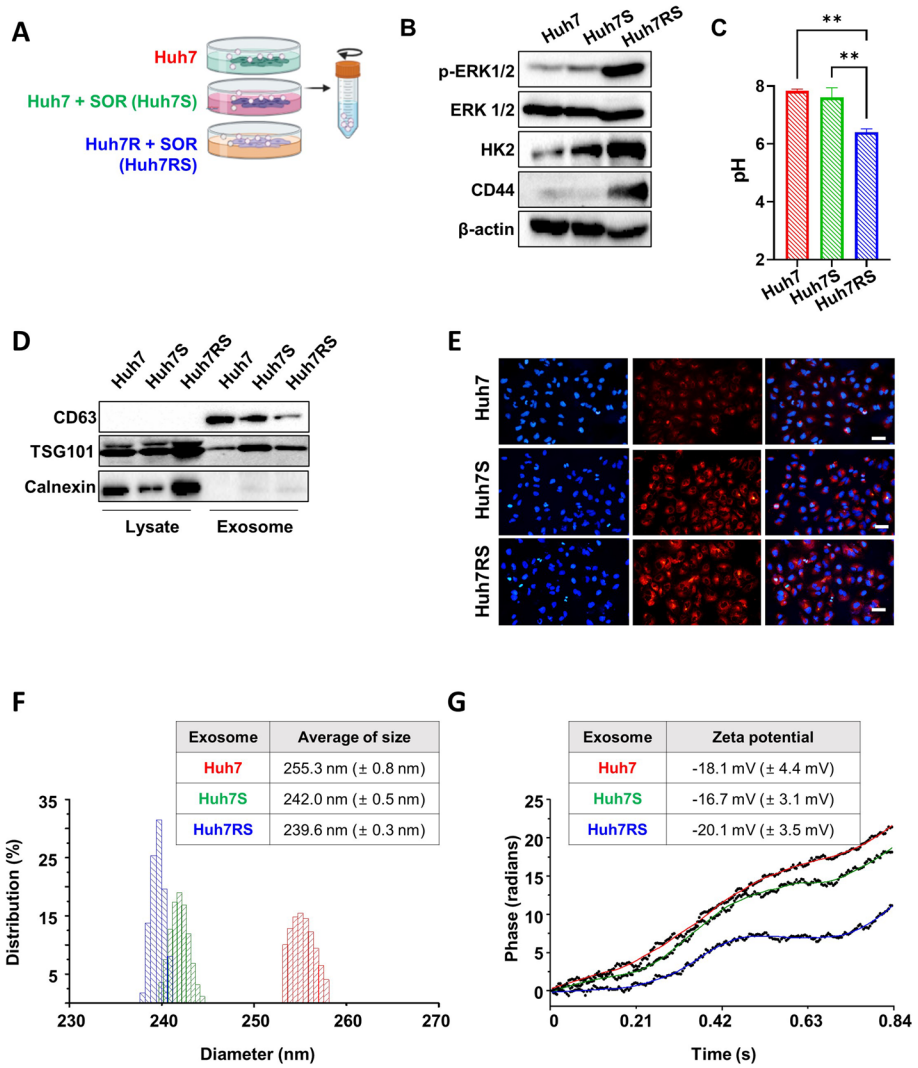

Fig. 1 Characterization of isolated exosomes with exosomal markers and identification of cellular internalization of EV-labeled exosomes. **A** Schematic of experimental conditions. **B** Western blot demonstrating the protein expression levels of phospho-ERK 1/2 (p-ERK 1/2), ERK 1/2, hexokinase II (HK2), CD44, and β-actin in Huh7, Huh7S and Huh7RS cells. Densitometry intensity ratio of (**A**) from replicated western blots ($n=3$) is shown in Additional file 1: Fig. S2. The full-length blots are in Additional file 2: Fig. S1. (**C**) The level of pH in Huh7, Huh7S and Huh7RS cells. After plating cells for 24 h, the level of pH was measured using pHrodo dye ($n=6$). The results are presented as the mean ± SD; $^{**}p<0.01$; $^{***}p<0.001$. (**D**) Expression levels of the exosome-positive (CD63, TSG101) and negative (Calnexin) markers in cell lysate and exosomes from Huh7, Huh7S, and Huh7RS cells assessed using western blotting. Cells were incubated in exosome-depleted medium supplemented with or without 20 μM sorafenib. After 24 h, exosomes were isolated from Huh7, sorafenib-treated Huh7 (Huh7S), and sorafenib-treated Huh7 resistant cells (Huh7RS). The full-length blots are shown in Additional file 2: Fig. S2 (**E**) Under the same conditions as in (**D**). EV-membrane of the isolated exosomes were labeled with a fluorescent dye and administered to the target cells. After DAPI-staining, the uptake of exosomes by the target cells was observed using fluorescence microscopy. Scale bar: 50 μm. **F**, **G** Dynamic light scattering (DLS) and zeta potential (**G**) measured using ZetaPALS®. Exosome samples were mixed and diluted to a final volume of 2 mL with PBS and zeta potential was analyzed using the Smoluchowski model

These findings suggest that the abnormal expression of exosomal miRNAs may be attributed to the miRNAs present in Huh7 and Huh7R cells.

Role of miR-6126 dysregulation in sorafenib resistance in sorafenib-resistant Huh7 cells

Despite miR-6126 being a tumor suppressor gene, very little is known about its role in HCC, particularly regarding sorafenib resistance. To investigate the role of miR-6126, Huh7R cells with the lowest expression of miR-6126 were transfected with an miR-6126 mimic. Increased expression of miR-6126 was confirmed using RT-PCR (Fig. 4A). Huh7R cells with upregulated miR-6126 expression exhibited a significant reduction in cell viability compared to negative control (NC)-transfected Huh7R cells, indicating that miR-6126 expression levels

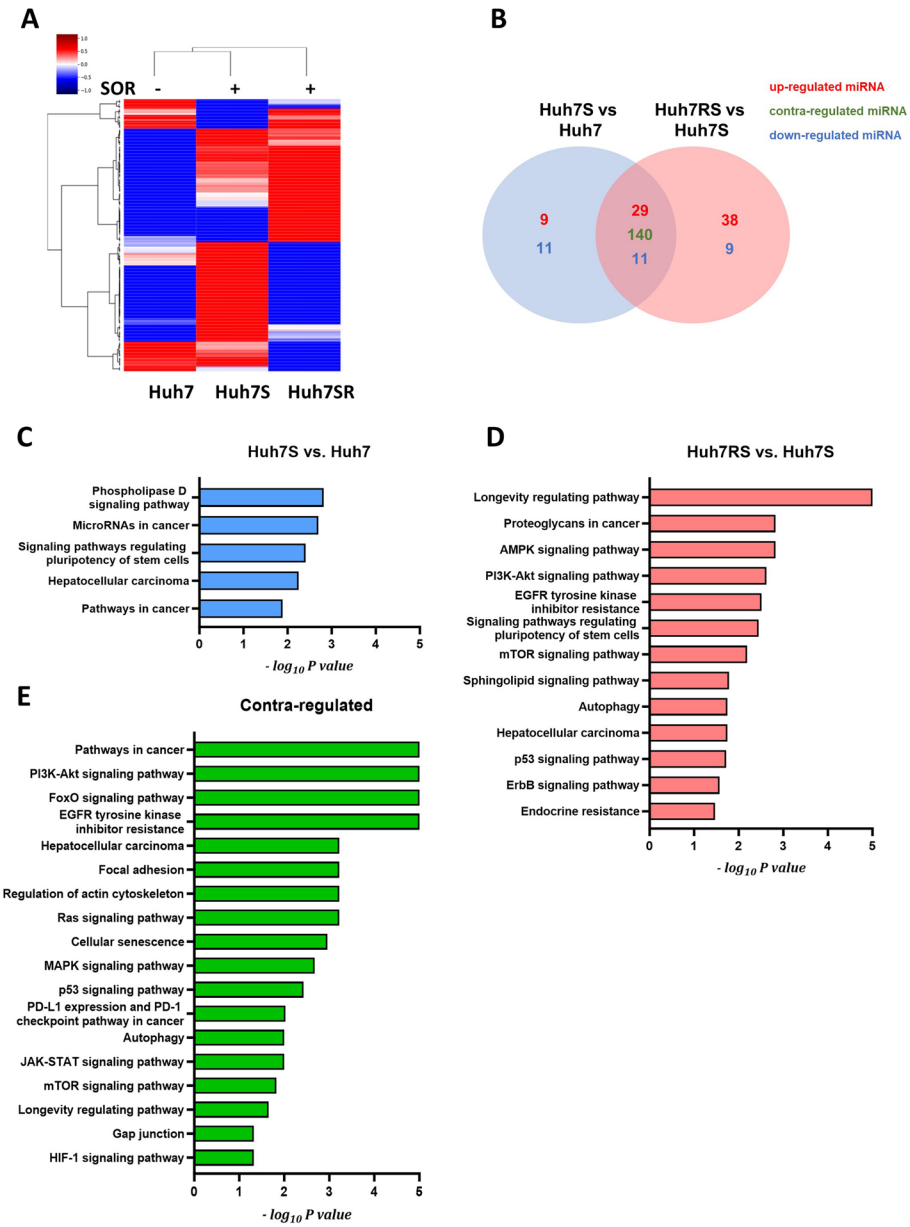

Fig. 2 Differential miRNA expression in exosomes from Huh7, Huh7S, and Huh7RS cells determined using miRNA microarray. **A** Heatmap illustrating the microarray expression analysis of all exosomal miRNAs detected in exosomes from Huh7, Huh7S, and Huh7SR (fold change > 1.5). **B** Venn diagram representing differential expression profiles of exosomal miRNA from Huh7, Huh7S, and Huh7SR cells. **C**–**E** The top enriched KEGG pathways for target genes of dysregulated exosomal miRNAs between Huh7S and Huh7 (**C**) and between Huh7SR and Huh7S (**D**). The top enriched KEGG pathways for target genes of contra-dysregulated miRNAs (**E**) between (**C**) and (**E**). Huh7S, sorafenib-treated Huh7 cells; Huh7RS, sorafenib-treated Huh7R cells

are associated with sorafenib resistance (Fig. 4B). Following the transfection of Huh7R cells with the miR-6126 mimic, we evaluated the proteins upregulated in Huh7R cells compared to Huh7 cells. Notably, the elevated levels of phospho-ERK 1/2 (p-ERK 1/2) and the glycolysis-related protein HK2 were diminished in Huh7R cells overexpressing miR-6126 after sorafenib treatment (Additional File 1; Fig. S4A). Similarly, the recovery of sorafenib resistance through miR-6126 was confirmed in SK-Hep1R cells overexpressing miR-6126 (Additional File 1; Fig. S4B and S4C).

Additionally, Huh7R cells with miR-6126 overexpression displayed a higher pH level after sorafenib treatment compared to the negative control group (Fig. 4C). This

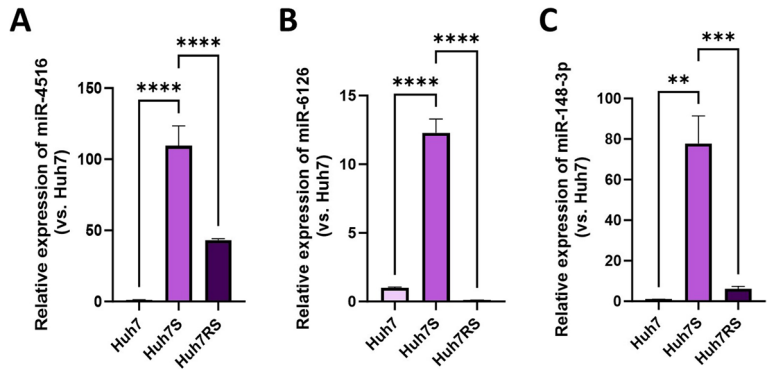

Fig. 3 Expression levels of miR-4516, miR-6126, and miR-148-3p in Huh7-, Huh7S-, and Huh7RS- derived exosomes. **A**-**C** Expression levels of miR-4516 (**A**), miR-6126 (**B**), and miR-148a-3p (**C**) determined by RT-qPCR using exosomal miRNA from Huh7, Huh7S, and Huh7RS cells. The expression level of each target miRNA was normalized using that of rRNA using the $2^{-\Delta\Delta Ct}$ method (**$P < 0.01$; ***$P < 0.001$; ****$P < 0.0001$)

elevated pH influences the expression of cancer stem cell markers (Ref 8–9). Notably, CD44, a well-known cancer stem cell marker, exhibited reduced expression in Huh7R cells overexpressing the miR-6126 mimic (Fig. 4D). To further validate the role of miR-6126 in sorafenib-resistant HCC cells, we employed 3D spheroids derived from Huh7R cells. Consistent with the findings from 2D cultures, we observed a greater reduction in spheroid size and in the expression of Ki67, a proliferation marker (Fig. 4E-H).

To verify the role of miR-6126, Huh7 cells expressing the highest levels of miR-6126 were treated with an miR-6126 inhibitor. Reduced expression of miR-6126 was confirmed using RT-PCR (Fig. 5A). Huh7 cells with downregulated miR-6126 expression exhibited reduced sensitivity to sorafenib compared to control Huh7 cells, suggesting that the expression level of miRNA-6126 affects sorafenib sensitivity (Fig. 5B). The expression levels of p-ERK 1/2 and HK2 were increased in sorafenib-treated Huh7 cells after treatment with miR-6126 inhibitor (Additional File 1; Fig S4F). In contrast to Huh7 cells treated with the miR-6126 mimic, Huh7 cells treated with the miR-6126 inhibitor showed a lower pH level after sorafenib treatment compared to the negative control group (Fig. 5C). Additionally, CD44 expression was increased in Huh7 cells treated with the miR-6126 inhibitor (Fig. 5D). The miR-6126 inhibitor-treated Huh7 cells did not exhibit a reduction in spheroid size after sorafenib treatment (Fig. 5E, F). Together, these findings demonstrate that miR-6126 plays a pivotal role in regulating sorafenib sensitivity and the expression of tumor-associated proteins.

Role of exosomal miR-6126 in Huh7R cells

Next, we assessed the effect of miR-6126 levels on sorafenib resistance in Huh7R cells. After transfection of the miR-6126 mimic into Huh7R cells, exosomal miRNAs were extracted to generate exosomes containing high levels of miR-6126, as confirmed using RT-PCR (Fig. 6A). Sorafenib treatment significantly reduced the viability of miR-6126-enriched exosome-treated Huh7R cells compared to that in control exosome- treated Huh7R cells (Fig. 6B). Consistent with previous findings, Huh7R cells treated with miR-6126-enriched exosomes exhibited decreased levels of p-ERK 1/2, ERK 1/2, HK2, and CD44 compared with those treated with control exosomes (Fig. 6C and Additional File 1; Fig. S5). These results indicate that exosomal miR-6126 modulates sorafenib resistance and tumorigenesis.

Discussion

Sorafenib is widely recognized as the first-line treatment for patients with advanced HCC. However, significant challenges remain due to the severe side effects and the development of acquired resistance by tumor cells. Increasing evidence underscores the critical role of cancer cell-derived miRNAs in modulating drug resistance. Through the analysis of exosomal miRNAs expressed at significantly altered levels in sorafenib-resistant HCC cells compared to control cells, we identified a novel miRNA that regulates cancer metabolism and inhibits tumorigenesis. Specifically, we investigated the effects of miR-6126 on drug resistance in sorafenib-treated HCC cells and found that exosomes enriched with miR-6126 significantly enhanced the therapeutic efficacy of sorafenib in sorafenib-resistant Huh7 cells.

Exosomes serve as vehicles for diverse active biological cargo, including proteins, mRNAs, miRNAs, and other non-coding RNAs, thereby influencing the characteristics of recipient cells [4, 21]. miRNA-laden exosomes derived from tumor cells have been implicated in tumor progression through the modulation of anti-tumor

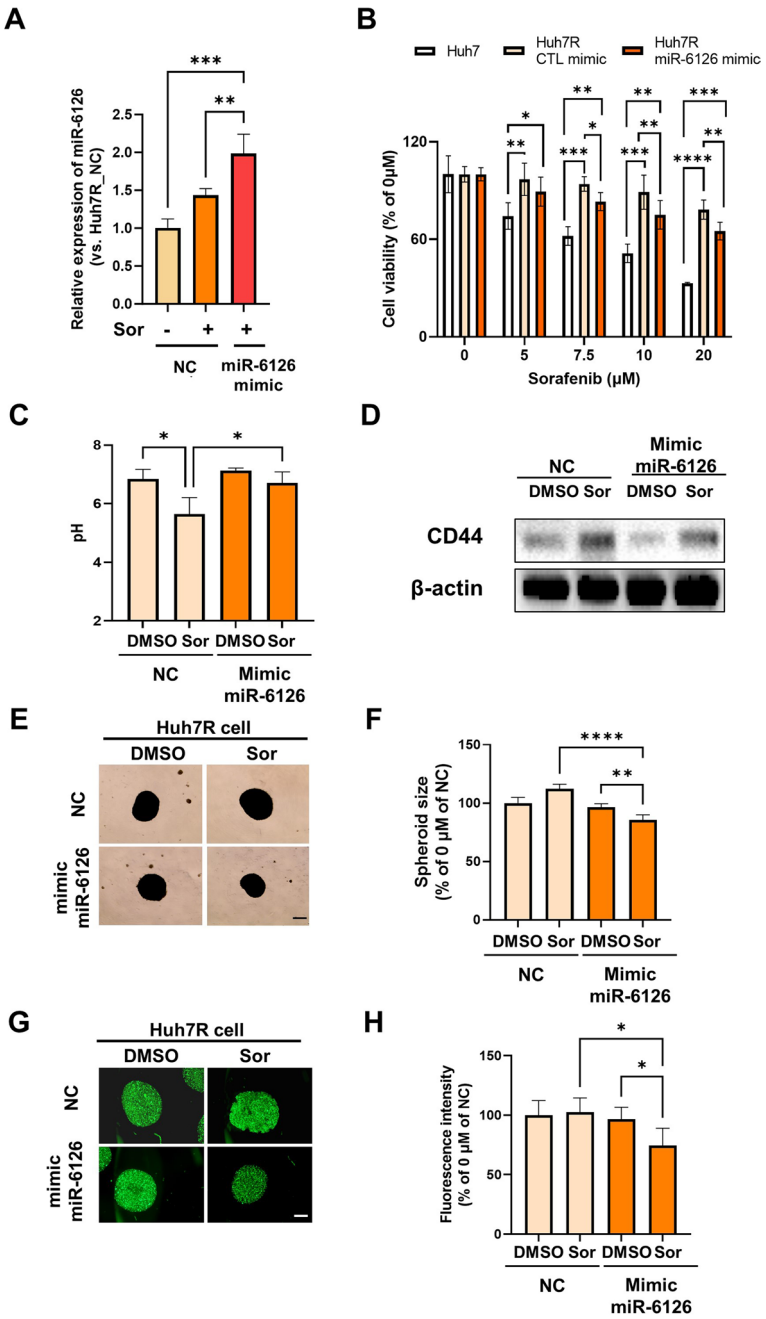

Fig. 4 Regulation of sorafenib resistance after miR-6126 modulation. **A** Expression level of miR-6126 evaluated using RT-qPCR. For expression analysis using RT-PCR, Huh7R cells were transfected with 500 pM of negative control (NC) or miR-6126 mimic for 72 h, followed by treatment with 20 μM sorafenib (SOR) for 48 h. rRNA was used to normalize the results using the $2^{-\Delta\Delta Ct}$ method. **B** Viability of Huh7 and Huh7R cells transfected with either an NC or a miR-6126 mimic measured after treatment with the indicated concentrations of SOR for 48 h. **C** The level of pH in negative control (NC) or mimic miR-6126 overexpressing Huh7R cells after DMSO or sorafenib (SOR) treatment. The level of pH was measured using pHrodo dye ($n=6$). Data represent the mean ± SD; *$p<0.05$. **D** Expression levels of CD44, and β-actin analyzed using western blotting. The full-length blots are shown in Additional file 2: Fig. S3. **E** Representative images of spheroids after 48 h of transfection with either the negative control (NC) or miR-6126 mimic, followed by sorafenib treatment. Images were acquired using an inverted microscope. Scale bar: 100 μm. **F** The relative change in spheroid size ($n=3$ for each of the three independent experiments) was quantified using Olympus CellSens software. Data are presented as the mean ± SD. **$p<0.01$, ****$p<0.0001$. **G** Representative Ki67 immunostaining of spheroids from panel (**E**). Spheroids were fixed with 2% paraformaldehyde (PFA) and stained. Images were acquired using an Olympus BX53 microscope. Scale bar: 200 μm. **H** Ki67 fluorescence intensity was measured using Olympus CellSens software. Data are presented as the mean ± SD. *$p<0.05$

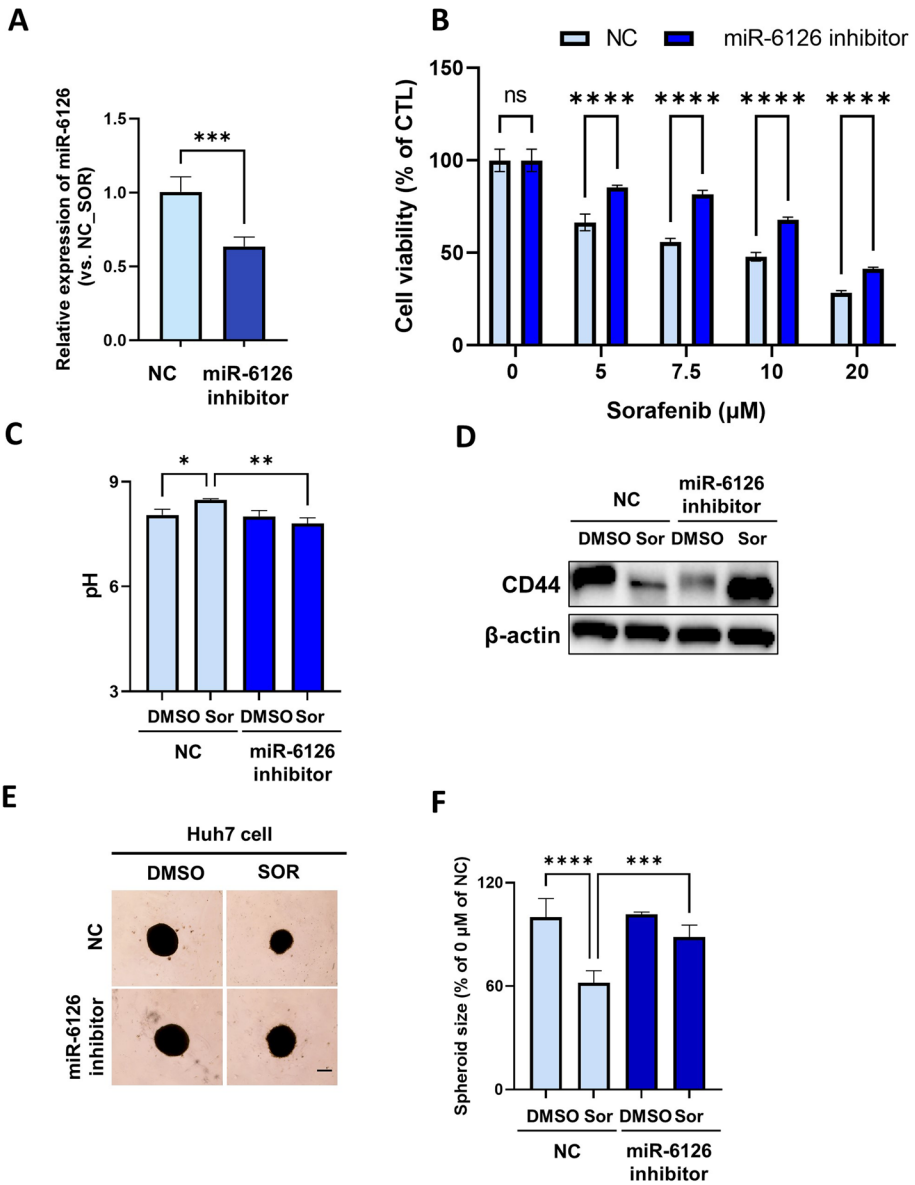

Fig. 5 Increased sorafenib resistance after miR-6126 inhibitor treatment. **A** Expression level of miR-6126 evaluated using RT-qPCR. For expression analysis using RT-PCR, Huh7 cells were transfected with 100 nM negative control (NC) or miR-6126 inhibitor for 72 h. rRNA was used to normalize the results using the $2^{-\Delta\Delta Ct}$ method. **B** Viability of Huh7 cells treated with 100 nM NC or miR-6126 inhibitors, after being treated with indicated concentrations of SOR for 48 h. **C** The pH level in NC or miR-6126 inhibitor-treated Huh7 cells was measured after treatment with DMSO or sorafenib (SOR). The pH level was assessed using pHrodo dye ($n=6$). Data show the mean ± SD; *$p<0.05$ **D** Expression levels of CD44, and β-actin analyzed using western blotting. The full-length blots are shown in Additional file 2; Fig. S4. **E** Representative images of spheroids after 48 h of treatment with either the NC or miR-6126 inhibitor, followed by sorafenib treatment. Images were acquired using an inverted microscope. Scale bar: 100 μm. **F** The relative change in spheroid size ($n=3$ for each of the three independent experiments) was quantified using Olympus CellSens software. Data are presented as the mean ± SD. ***$p<0.001$, ****$p<0.0001$

effects [22, 23]. For example, Dong et al. demonstrated that miR-124-3p.1 enhances the efficacy of sorafenib in liver cancer cells via the FoxO3A axis [24]. Similarly, Xu et al. reported that combined treatment with sorafenib and miR-367-3p elevated the anti-cancer effects of sorafenib, leading to suppressed cell invasion both in vivo and in vitro, mediated by the ERK pathway [25]. Furthermore, dysregulation of miR-30d expression has been observed in patients with sorafenib-resistant HCC [26]. Our exosomal miRNA analysis comparing Huh7 and Huh7RS cells, as well as Huh7S and Huh7RS cells, identified 247 dysregulated miRNAs in these groups. Notably,

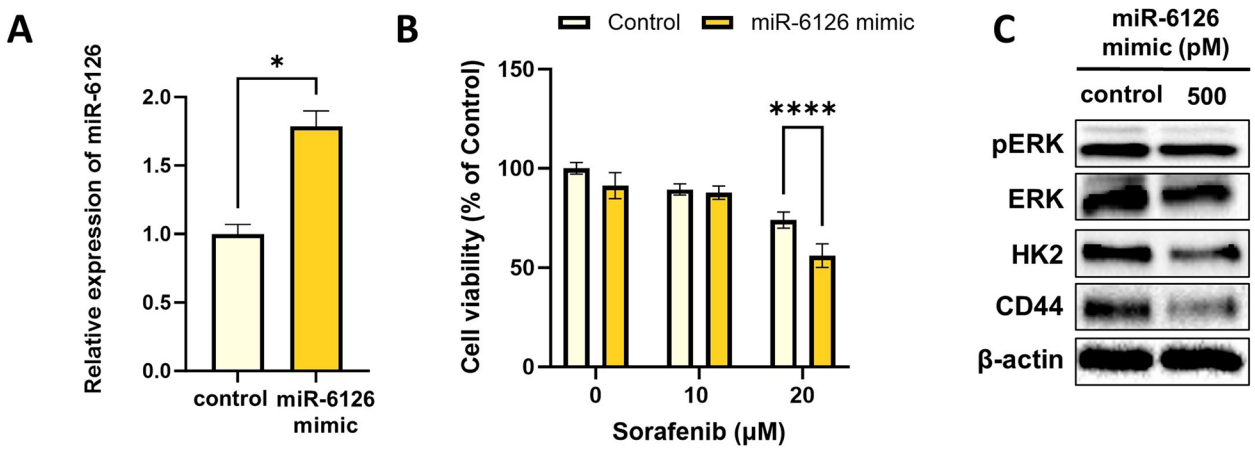

Fig. 6 Effect of exosomal miR-6126 on Huh7R cells. **A** Expression level of miR-6126 assessed using real-time qPCR. Huh7R cells were transfected with 500 pM NC or miR-6126 mimic for 24 h and the medium was replaced by exosome-depleted medium. After 48 h of incubation, exosomes were isolated from each cell culture medium and used for real-time qPCR. The result was normalized to that of rRNA using the $2^{-\Delta\Delta Ct}$ method (***$P < 0.001$). **B** Proliferation of Huh7R cells treated with exosomes isolated in (**A**) and incubated for 18 h, followed by treatment with the indicated concentrations of sorafenib for 48 h (*$P < 0.05$). **C** Expression levels of p-ERK1/2, ERK 1/2, HK2, CD44 and β-actin in Huh7R cells treated with exosomes isolated in (**A**). Huh7R cells treated with exosomes were incubated for 18 h, and subsequently, treated with (SOR; 20 μM) or without sorafenib (NOR) and incubated for 48 h. Expression levels of the protein were measured using western blotting. Densitometry intensity ratio of (**C**) from replicated western blots ($n = 3$) and full-length blots are shown in Additional file 2: Fig. S5 Additional Files Additional file 1: Table S1, Fig. S1–Fig. S5 Additional file 2: Fig. S1–Fig. S5

our study focused specifically on Huh7S cells to pinpoint miRNAs directly involved in sorafenib resistance. Indeed, the comparison between Huh7 and Huh7S cells revealed dysregulation of 20 miRNAs, which were subsequently excluded from further analysis. In a recent study, an evaluation of the drug sensitivity in 14 different HCC cell lines identified Huh7 as one of the most sensitive HCC cell lines to sorafenib [20]. This sensitivity makes Huh-7 an excellent model for studying sorafenib resistance, as it may identify miRNAs and other molecular factors involved in the development of resistance in a previously sensitive cell line.

Among the differentially expressed exosomal miRNAs between Huh7 and Huh7S cells and Huh7S and Huh7RS cells, we focused on three exosomal miRNAs, namely miR-6126, miR-4516, and miR-148-3p. Among these, miR-4516 exhibited varying effects on different tumor types. Increased levels of miR-4516 inhibit tumor cell proliferation and migration, as observed in HCC and pancreatic cancer cells [27–29]. In contrast, downregulation of miR-4516 was observed in colorectal cancer and retinoblastoma tumors [30, 31]. miR-148-3p is known to inhibit tumor progression in HCC, gastric cancer, and esophageal cancer [32–34]. Regarding, miR-6126, recent studies suggest that upregulation of exosomal miR-6126 inhibits cell proliferation and tumor metastasis by regulating the PI3K/AKT signaling pathway through the interference of integrin β−1 in ovarian cancer [35]. Nevertheless, few studies have explored its function in tumorigenesis and resistance to anti-cancer drugs. In the present study, we demonstrated that upregulation of both miR-6126 and exosomal miR-6126 inhibited the expression of p-ERK1/2, glycolysis-related proteins (HK2), and stem cell-related proteins (CD44). These findings are consistent with those of previous studies; however, only a few miRNAs associated with stem cells in HCC have been identified. For instance, miR-192-5p has been identified as a regulator of CSC-related features, with decreased expression observed in HCC cells expressing high levels of CSC markers [36]. Conversely, miR-106b-5p promotes cancer metastasis and cell proliferation in HCC by upregulating CSC biomarkers by targeting PTEN in the PI3K/AKT pathway [37]. Our findings revealed a reduction in CD44 levels following the transfection of Huh7R cells with the miR-6126 mimic. CD44 is known to promote progression, migration, and extrahepatic metastasis via AKT/ERK signaling [38, 39]. CD44 also enhances the glycolytic phenotype through its interaction with pyruvate kinase M2 in cancer cells [40]. Furthermore, a higher distribution of CD44-positive cells has been reported among sorafenib-resistant populations [41]. Together, our findings suggest that the modulation of exosomal miR-6126 could represent a potential therapeutic target for CD44-positive cells, which are associated with poor prognosis in patients with HCC. However, a limitation of this study was the lack of predictive analysis regarding the binding sites of miR-6126 on CD44. As we were unable to confirm this through target prediction software, we

hypothesized that CD44 is indirectly regulated by other proteins. Nevertheless, future research should focus on elucidating these regulatory mechanisms.

In conclusion, our study highlights the persistent challenges of sorafenib resistance in HCC treatment. By elucidating the role of exosomal miR-6126 in both sorafenib resistance and tumorigenesis, we propose that miR-6126 represents a promising and innovative therapeutic target for addressing sorafenib-resistant HCC. This work opens potential avenues for developing more effective and targeted treatment strategies in the ongoing battle against this challenging disease.

Abbreviations

HCC	hepatocellular carcinoma
miRNA	microRNA
PDGFR	platelet-derived growth factor receptor
VEGFR	vascular endothelial growth factor receptor
HK2	hexokinase II
LDHA	lactate dehydrogenase A
EV	extracellular vesicles

Supplementary Information

The online version contains supplementary material available at https://doi.org/10.1186/s12885-024-13342-y.

Additional file 1: Table S1, Fig. S1–Fig. S5.

Additional file 2: Fig. S1–Fig. S5.

Acknowledgements
Not applicable.

Authors' contributions
M.Lee conceived and designed all the experiments. H.H, J.K performed the experiments, collected and analyzed the data, and wrote the manuscript. T.K, Y.H, D.C, S.C, S.K, S.P, and T.P performed the experiments and the data analysis. F.P, W.R and J.P interpreted the results. All authors critically reviewed and approved the final manuscript.

Funding
This research was supported by the National Research Foundation of Korea (Seoul, Korea; grant numbers NRF-2022R1A2C1007956) and by Research Project Support Program for Excellence Institute in Incheon National University.

Data availability
Data is provided within the manuscript or supplementary information files.

Declarations

Ethics approval and consent to participate
Not applicable.

Consent for publication
Not applicable.

Competing interests
The authors declare no competing interests.

Author details
[1]Division of Life Sciences, College of Life Science and Bioengineering, Incheon National University, Incheon 22012, Republic of Korea. [2]Department of Materials Science and Engineering, Yonsei University, 50 Yonsei-Ro, Seodaemun-Gu, Seoul 03722, Republic of Korea. [3]IRCCS Istituto Romagnolo per lo Studio dei Tumori (IRST) "Dino Amadori", Meldola, Italy. [4]Department of Medical and Surgical Sciences (DIMEC), University of Bologna, Bologna, Italy. [5]Department of Bioengineering and Nano-Bioengineering, Incheon National University, Incheon 22012, Republic of Korea. [6]Institute for New Drug Development, College of Life Science and Bioengineering, Incheon National University, Incheon 22012, Republic of Korea.

Received: 6 February 2024 Accepted: 12 December 2024
Published online: 20 December 2024

References

1. Sia D, Villanueva A, Friedman SL, Llovet JM. Liver Cancer Cell of Origin, Molecular Class, and Effects on Patient Prognosis. Gastroenterology. 2017;152(4):745–61.
2. Llovet JM, Zucman-Rossi J, Pikarsky E, Sangro B, Schwartz M, Sherman M, Gores G. Hepatocellular carcinoma. Nat Rev Dis Primers. 2016;2:16018.
3. Adnane L, Trail PA, Taylor I, Wilhelm SM. Sorafenib (BAY 43–9006, Nexavar), a dual-action inhibitor that targets RAF/MEK/ERK pathway in tumor cells and tyrosine kinases VEGFR/PDGFR in tumor vasculature. Methods Enzymol. 2006;407:597–612.
4. Wilhelm SM, Carter C, Tang L, Wilkie D, McNabola A, Rong H, et al. BAY 43-9006 exhibits broad spectrum oral antitumor activity and targets the RAF/MEK/ERK pathway and receptor tyrosine kinases involved in tumor progression and angiogenesis. Cancer Res. 2004;64(19):7099–109.
5. Tanaka S, Arii S. Molecular targeted therapies in hepatocellular carcinoma. Semin Oncol. 2012;39(4):486–92.
6. Abou-Alfa GK, Schwartz L, Ricci S, Amadori D, Santoro A, Figer A, et al. Phase II study of sorafenib in patients with advanced hepatocellular carcinoma. J Clin Oncol. 2006;24(26):4293–300.
7. Tang W, Chen Z, Zhang W, Cheng Y, Zhang B, Wu F, et al. The mechanisms of sorafenib resistance in hepatocellular carcinoma: theoretical basis and therapeutic aspects. Signal Transduct Target Ther. 2020;5(1):87.
8. Vander Heiden MG, Cantley LC, Thompson CB. Understanding the Warburg effect: the metabolic requirements of cell proliferation. Science. 2009;324(5930):1029–33.
9. Webb BA, Chimenti M, Jacobson MP, Barber DL. Dysregulated pH: a perfect storm for cancer progression. Nat Rev Cancer. 2011;11(9):671–7.
10. DeBerardinis RJ, Mancuso A, Daikhin E, et al. Beyond aerobic glycolysis: transformed cells can engage in glutamine metabolism that exceeds the requirement for protein and nucleotide synthesis. Proc Natl Acad Sci U S A. 2007;104(49):19345–50.
11. Xin HW, Ambe CM, Hari DM, Wiegand GW, Miller TC, Chen JQ, et al. Label-retaining liver cancer cells are relatively resistant to sorafenib. Gut. 2013;62(12):1777–86.
12. Cully M. Exosome-based candidates move into the clinic. Nat Rev Drug Discov. 2021;20(1):6–7.
13. Ela S, Mager I, Breakefield XO, Wood MJ. Extracellular vesicles: biology and emerging therapeutic opportunities. Nat Rev Drug Discov. 2013;12(5):347–57.
14. Fang JH, Zhang ZJ, Shang LR, Luo YW, Lin YF, Yuan Y, et al. Hepatoma cell-secreted exosomal microRNA-103 increases vascular permeability and promotes metastasis by targeting junction proteins. Hepatology. 2018;68(4):1459–75.
15. Xiao X, Yu S, Li S, Wu J, Ma R, Cao H, et al. Exosomes: decreased sensitivity of lung cancer A549 cells to cisplatin. PLoS ONE. 2014;9(2):e89534.
16. Ji L, Lin Z, Wan Z, Xia S, Jiang S, Cen D, et al. miR-486-3p mediates hepatocellular carcinoma sorafenib resistance by targeting FGFR4 and EGFR. Cell Death Dis. 2020;11(4):250.
17. Feng X, Zou B, Nan T, Zheng X, Zheng L, Lan J, et al. MiR-25 enhances autophagy and promotes sorafenib resistance of hepatocellular carcinoma via targeting FBXW7. Int J Med Sci. 2022;19(2):257–66.
18. Fornés JA. The Smoluchowski Model. In: Principles of Brownian and Molecular Motors. Springer Series in Biophysics, Springer, Cham. 2021;21:49–63.
19. Sung JS, Han Y, Yun TG, et al. Monocarboxylate transporter-1 (MCT-1) inhibitors screened from autodisplayed FV-antibody library. Int J Biol Macromol. 2024;265(Pt 1):130854.
20. Gao R, Tang F, Christofori G. Protocol to screen for Sorafenib resistance regulators using pooled lentiviral shRNA library and a Sorafenib-resistant hepatocellular carcinoma cell model. STAR Protoc. 2023;4(2):102273.

21. Valadi H, Ekstrom K, Bossios A, Sjostrand M, Lee JJ, Lotvall JO. Exosome-mediated transfer of mRNAs and microRNAs is a novel mechanism of genetic exchange between cells. Nat Cell Biol. 2007;9(6):654–9.
22. Santos P, Almeida F. Role of exosomal miRNAs and the tumor microenvironment in drug resistance. Cells. 2020;9(6):1450.
23. Guo QR, Wang H, Yan YD, Liu Y, Su CY, Chen HB, et al. The role of exosomal microRNA in cancer drug resistance. Front Oncol. 2020;10:472.
24. Dong ZB, Wu HM, He YC, Huang ZT, Weng YH, Li H, et al. miRNA-124-3p.1 sensitizes hepatocellular carcinoma cells to sorafenib by regulating FOXO3a by targeting AKT2 and SIRT1. Cell Death Dis. 2022;13(1):35.
25. Xu J, Lin H, Li G, Sun Y, Chen J, Shi L, et al. The miR-367-3p increases sorafenib chemotherapy efficacy to suppress hepatocellular carcinoma metastasis through altering the androgen receptor signals. EBioMedicine. 2016;12:55–67.
26. Kohno T, Morishita A, Iwama H, Fujita K, Tani J, Takuma K, et al. Comprehensive analysis of circulating microRNAs as predictive biomarkers for sorafenib therapy outcome in hepatocellular carcinoma. Oncol Lett. 2020;20(2):1727–33.
27. Li Q, Wang W, Yang T, Li D, Huang Y, Bai G, et al. LINC00520 up-regulates SOX5 to promote cell proliferation and invasion by miR-4516 in human hepatocellular carcinoma. Biol Chem. 2022;403(7):665–78.
28. Li O, Li Z, Tang Q, Li Y, Yuan S, Shen Y, et al. Long stress induced non-coding transcripts 5 (LSINCT5) promotes hepatocellular carcinoma progression through interaction with high-mobility group AT-hook 2 and miR-4516. Med Sci Monit. 2018;24:8510–23.
29. Chen S, Xu M, Zhao J, Shen J, Li J, Liu Y, et al. MicroRNA-4516 suppresses pancreatic cancer development via negatively regulating orthodenticle homeobox 1. Int J Biol Sci. 2020;16(12):2159–69.
30. Wang Z, Xu R. lncRNA PART1 promotes breast cancer cell progression by directly targeting miR-4516. Cancer Manag Res. 2020;2:7753–60.
31. Jin XH, Lu S, Wang AF. Expression and clinical significance of miR-4516 and miR-21-5p in serum of patients with colorectal cancer. BMC Cancer. 2020;20(1):241.
32. Wang Y, Hu Y, Guo J, Wang L. miR-148a-3p suppresses the proliferation and invasion of esophageal cancer by targeting DNMT1. Genet Test Mol Biomarkers. 2019;23(2):98–104.
33. Li B, Wang W, Li Z, Chen Z, Zhi X, Xu J, et al. MicroRNA-148a-3p enhances cisplatin cytotoxicity in gastric cancer through mitochondrial fission induction and cyto-protective autophagy suppression. Cancer Lett. 2017;410:212–27.
34. Huang Z, Wen J, Yu J, Liao J, Liu S, Cai N, et al. MicroRNA-148a-3p inhibits progression of hepatocellular carcinoma by repressing SMAD2 expression in an Ago2 dependent manner. J Exp Clin Cancer Res. 2020;39(1):150.
35. Kanlikilicer P, Rashed MH, Bayraktar R, Mitra R, Ivan C, Aslan B, et al. Ubiquitous release of exosomal tumor suppressor miR-6126 from ovarian cancer cells. Cancer Res. 2016;76(24):7194–207.
36. Gu Y, Wei X, Sun Y, Gao H, Zheng X, Wong LL, et al. miR-192-5p silencing by genetic aberrations is a key event in hepatocellular carcinomas with cancer stem cell features. Cancer Res. 2019;79(5):941–53.
37. Shi DM, Bian XY, Qin CD, Wu WZ. miR-106b-5p promotes stem cell-like properties of hepatocellular carcinoma cells by targeting PTEN via PI3K/Akt pathway. Onco Targets Ther. 2018;11:575–85.
38. Herishanu Y, Gibellini F, Njuguna N, Hazan-Halevy I, Farooqui M, Bern S, et al. Activation of CD44, a receptor for extracellular matrix components, protects chronic lymphocytic leukemia cells from spontaneous and drug induced apoptosis through MCL-1. Leuk Lymphoma. 2011;52(9):1758–69.
39. Huang C, Yoon C, Zhou XH, Zhou YC, Zhou WW, Liu H, et al. ERK1/2-Nanog signaling pathway enhances CD44(+) cancer stem-like cell phenotypes and epithelial-to-mesenchymal transition in head and neck squamous cell carcinomas. Cell Death Dis. 2020;11(4):266.
40. Tamada M, Nagano O, Tateyama S, Ohmura M, Yae T, Ishimoto T, et al. Modulation of glucose metabolism by CD44 contributes to antioxidant status and drug resistance in cancer cells. Cancer Res. 2012;72(6):1438–48.
41. Chow AK, Ng L, Lam CS, Wong SK, Wan TM, Cheng NS, et al. The enhanced metastatic potential of hepatocellular carcinoma (HCC) cells with sorafenib resistance. PLoS ONE. 2013;8(11):e78675.

Publisher's Note